



# Study of electrical and electrochemical behavior on copper ion conducting nano-composite polymer electrolyte

Tripti Bala Sahu<sup>1</sup> · Manju Sahu<sup>1</sup> · Shrabani Karan<sup>1</sup> · Y. K. Mahipal<sup>1</sup> · D. K. Sahu<sup>2</sup> · R. C. Agrawal<sup>1</sup>

Received: 23 August 2017 / Revised: 21 November 2017 / Accepted: 2 December 2017 / Published online: 19 December 2017  
© Springer-Verlag GmbH Germany, part of Springer Nature 2017

## Abstract

Poly (ethylene oxide) (PEO)-based nano-composite polymer electrolyte (NCPE) membranes: [85PEO: 15Cu(ClO<sub>4</sub>)<sub>2</sub>·6H<sub>2</sub>O] + *x* Al<sub>2</sub>O<sub>3</sub>, where *x* = 0, 1, 2, 3, 4, 5, 6, 7, 8 wt%, have been casted by hot-press technique. Solid polymer electrolyte (SPE) composition: [85PEO: 15Cu(ClO<sub>4</sub>)<sub>2</sub>·6H<sub>2</sub>O] (wt%) is highest conducting film with room temperature conductivity ( $\sigma_{rt}$ ) ~  $1.59 \times 10^{-6}$  S/cm, has been used as the 1st-phase host matrix and Al<sub>2</sub>O<sub>3</sub> filler particles of nano-dimension (~ 50 nm) as 2nd-phase dispersoid. The fractional dispersal of Al<sub>2</sub>O<sub>3</sub> filler (viz. *x* = 2 wt%) in 1st-phase SPE host resulted into nearly four orders increase in the room temperature conductivity than that of pure PEO. This NCPE film: [85PEO: 15Cu (ClO<sub>4</sub>)<sub>2</sub>·6H<sub>2</sub>O] + 2 Al<sub>2</sub>O<sub>3</sub> has been referred to as optimum conducting composition (OCC) NCPE film. X-Ray diffraction (XRD), Fourier transform infrared (FTIR), scanning electron microscopy (SEM), differential scanning calorimetry (DSC), and Thermogravimetric Analysis (TGA) techniques have been used to study the structural, spectroscopic, morphological, and thermal responses, respectively, of SPE/NCPE OCC film material. The ion transport behavior has been characterized in terms of basic ionic parameters viz. conductivity ( $\sigma$ ), total ionic ( $t_{ion}$ )/cation ( $t_+$ ) transference numbers which have been evaluated using different ac/dc techniques. Temperature dependent conductivity measurement in SPE/NCPE OCC film was done in order to understand the mechanism of ion transport and to evaluate activation energy ( $E_a$ ) from “log  $\sigma$ -1/ $T$ ” plot.

**Keywords** Nano-composite polymer electrolyte (NCPE) · Hot-press technique · Ionic conductivity · Ionic transport number

## Introduction

Polymer electrolyte is an ion conducting membrane with moderate-high ionic conductivity ( $\sigma_{rt} \leq 10^{-4}$  Scm<sup>-1</sup>) at room temperature. The first ion conducting solid polymer electrolytes was reported in 1973 [1] and subsequently, the first solid polymer electrolyte (SPE)-based film battery was practically demonstrated in 1979 [2]. These novel discoveries inspired scientists/researchers both from academic institutions and industrial sectors to intensively pursue research in this area of Materials Science. Consequently, a large number of polymer electrolyte materials involving different kinds of transporting

ions, namely H<sup>+</sup>, Li<sup>+</sup>, Na<sup>+</sup>, K<sup>+</sup>, Ag<sup>+</sup>, and Mg<sup>2+</sup> have been reported. As already mentioned, the polymer electrolytes show great technological promise of fabricating a variety of all-solid-state electrochemical power sources, namely mini/macro primary/secondary batteries, fuel cells, and supercapacitors; hence, the applications of these materials in electrochemical devices are being explored extensively at different research and development laboratories as well as at commercial scales [1–20].

In the synthesis of SPE films, reported in the past, high mol. wt. polar polymer, namely poly (ethylene oxide) PEO has been commonly used as polymeric host matrix. The fact is that PEO possesses relatively higher electrochemical stability as well as an exceptional ability to dissolve wide variety of salts as compared to other polymers [2, 20]. The polar and flexible main chain dissociates the salt and hence, carrier ions are generated. These ions can migrate through the amorphous region of the polymer via inter-chain segmental motion. The degree of amorphosity of the polymer predominantly controls the ion conduction phenomenon in the polymer salt complexes. Larger is the amorphous region in the polymeric host,

✉ R. C. Agrawal  
rakesh\_c\_agrawal@yahoo.co.in

<sup>1</sup> Solid State Ionics Research Laboratory, School of Studies in Physics & Astrophysics, Pt. Ravishankar Shukla University, Raipur, Chhattisgarh 492010, India

<sup>2</sup> State Forensic Science Laboratory, Raipur 492001, India

higher would be the ionic conductivity. However, PEO-based SPEs often exhibit low ionic conductivity ( $10^{-4}$  S/cm) at room temperature, hence, not much useful for practical device applications. In order to solve such problems, various approaches of structural modifications have been adopted.

Dispersal of nano/micro-ceramic filler particles in SPE hosts also improves the morphological, electrochemical, and mechanical properties of the SPE membranes. The effects of dispersing filler particles of high conducting zeolites, ionites, and solid superacid sulfated-zirconia as well as insulating ceramic materials such as  $\text{Al}_2\text{O}_3$ ,  $\text{SiO}_2$ ,  $\text{TiO}_2$ ,  $\text{MgO}$ , and  $\text{CuO}$  on various physical/electrolytic properties of CPEs have been investigated by various workers [9–20]. Generally, the dispersal of a small fraction of filler particles in the polymer electrolytes enhances the ionic conductivity by 1–2 orders of magnitude. The enhancement in the conductivity is predominantly due to the increase of amorphous region in PEO as a consequence of the dispersal of the filler particles. Akin to 2-phase inorganic composite electrolytes [21], NCPEs are also 2-phase organic composite electrolytes in which SPE acts as Ist-phase host matrix and nanoparticles of filler material as IInd-phase dispersoid [20]. SPE/NCPE films are usually casted by the traditional solution cast method. However, an alternate procedure, popularly referred to as hot-press technique, has been developed for casting SPE/NCPE films [9–20]. This technique is recently getting wider acceptability due to the fact that it has several merits. It is cost-effective/more rapid and completely dry/solution-free film casting procedure as compare to the traditional solution cast method.

Today most of the modern portable rechargeable batteries available in the market are lithium batteries. However, these batteries reported to encounter several limitations, primarily due to use of lithium chemicals which are highly reactive/toxic especially in the open humid ambience. Moreover, these chemicals are very expensive due to low natural abundance as well as less environmental friendly. Hence, on account of high-priority safety concerns of battery while in operation, it was strongly felt to look for batteries free from lithium components. Attempts in this direction have been made in the recent years and some dry polymer electrolytes involving divalent cations viz.  $\text{Mg}^{2+}$ ,  $\text{Zn}^{2+}$ ,  $\text{Cu}^{2+}$  etc. as principal mobile species have been investigated [20, 28–37]. Complexing salts containing divalent cations possess several material advantages over lithium salts. They are relatively cheaper, high natural abundance, non-reactive, less toxic, environment friendly, etc. Moreover, divalent cations displace twice as much charge as monovalent cations. The present paper reports hot-press casting of NCPE membranes: [85PEO: 15Cu(ClO<sub>4</sub>)<sub>2</sub>.6H<sub>2</sub>O] + *x* Al<sub>2</sub>O<sub>3</sub>. SPE film composition: [85PEO: 15Cu(ClO<sub>4</sub>)<sub>2</sub>.6H<sub>2</sub>O] identified earlier having

highest ionic conductivity at room temperature has been used as Ist-phase host matrix and nano-particles (~ 50 nm) of Al<sub>2</sub>O<sub>3</sub> as IInd-phase dispersoid. Al<sub>2</sub>O<sub>3</sub>-dependent conductivity measurements on different films revealed the highest conducting film which has been referred to as optimum conducting composition (OCC) NCPE film.

The characterization of structural, spectroscopic, morphological, and thermal properties has been done using XRD, FTIR, SEM, and DSC techniques, respectively. The ion transport property has been studied in terms of basic ionic parameters viz. conductivity ( $\sigma$ ), total ionic ( $t_{\text{ion}}$ )/cation ( $t_+$ ) transference numbers which have been evaluated using different ac/dc techniques. Temperature-dependent conductivity measurement in SPE/NCPE OCC film was done in order to understand the mechanism of ion transport and to evaluate activation energy ( $E_a$ ) from “log  $\sigma$  to  $1/T$ ” plot.

## Experimental details

NCPE films: [85PEO: 15Cu(ClO<sub>4</sub>)<sub>2</sub>.6H<sub>2</sub>O] + *x* Al<sub>2</sub>O<sub>3</sub> in varying filler concentrations viz. *x* = 0, 1, 2, 3, 4, 5, 6, 7, 8 wt%, have been hot-press cast using AR grade precursor chemicals: Poly (ethylene oxide) PEO ( $6 \times 10^5$  Mw, purity > 99%, Aldrich, USA), Cu(ClO<sub>4</sub>)<sub>2</sub>.6H<sub>2</sub>O (> 98%, Aldrich, USA), and Al<sub>2</sub>O<sub>3</sub> (50 nm, Aldrich, USA). On the basis of composition-dependent conductivity study, a SPE composition of [85PEO: 15Cu(ClO<sub>4</sub>)<sub>2</sub>.6H<sub>2</sub>O] (85:15 wt%), identified as the highest conducting composition and was selected as polymer electrolyte host for dispersal of nano-sized Al<sub>2</sub>O<sub>3</sub> particles and hence, to prepare nano composite polymer electrolyte (NCPE) membranes using hot-press technique. Dry powders of SPE film composition: [85PEO: 15Cu(ClO<sub>4</sub>)<sub>2</sub>.6H<sub>2</sub>O], as Ist-phase host and Al<sub>2</sub>O<sub>3</sub> in different wt% ratios as IInd-phase were mixed physically for ~ 45 min. The homogeneous mixture was then heated close to melting point of PEO, i.e., ~ 70 °C for ~ 30–45 min with mixing continued. This gave rise to a soft slurry/lump, which was pressed (~ 1–2 ton/cm<sup>2</sup>) between two stainless steel (SS) blocks to form uniform thin film of thickness ~ 150–250 μm. As mentioned, filler particle concentration-dependent conductivity revealed NCPE OCC film. Temperature-dependent conductivity measurement was done on NCPE OCC film, and the activation energy ( $E_a$ ) was computed by least square linear fitting of “log  $\sigma$ – $1/T$ ” plot. The total ionic transference number ( $t_{\text{ion}}$ ) was determined by dc polarization transient ionic current (TIC) technique [22, 23]. The film sample, kept between SS (blocking) electrodes, was subjected to a fixed dc polarizing potential (V)~1 V, and the current were monitored as a function of time.  $T_{\text{ion}}$  was evaluated from ( $I_{\text{ion}}/I_T$ ) ratio obtained from “Current-Time” TIC plot. Cation (Cu<sup>2+</sup>) transport number ( $t_+$ ) was measured separately using a combined ac/dc technique [24]. The film

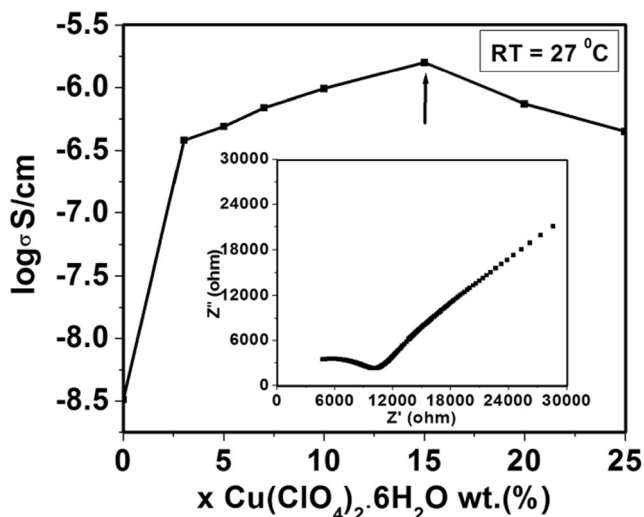


**Fig. 1** Salt concentration dependent conductivity variation for SPE films: [(1-x) PEO: x Cu(ClO<sub>4</sub>)<sub>2</sub>·6H<sub>2</sub>O]. (inset) Z''-Z' plot for SPE film: [85PEO: 15Cu(ClO<sub>4</sub>)<sub>2</sub>·6H<sub>2</sub>O]

sample, sandwiched between Cu (non-blocking) electrodes, was subjected to a fixed dc potential ΔV ~ 1 V, and t<sub>+</sub> was evaluated with the help of the following equation [24]:

$$t_+ = \frac{I_s(\Delta V - I_0 R_0)}{I_0(\Delta V - I_s R_s)} \quad (1)$$

where, I<sub>0</sub>/I<sub>s</sub> and R<sub>0</sub>/R<sub>s</sub> are initial/final current/resistance values before/after polarization which were obtained from dc polarization “current-time” and complex impedance Z''-Z' impedance plots, respectively.

The structural, spectroscopic, morphological, and thermal properties of the film material have been characterized, respectively, using viz. XRD (D<sub>2</sub> Phaser Model: 08 discover,

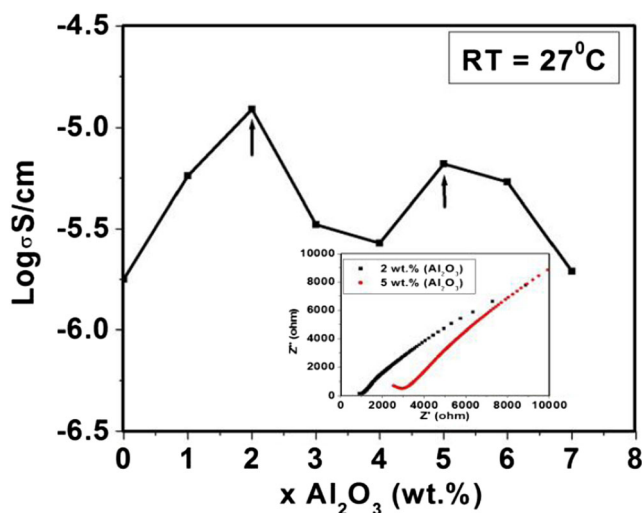


**Fig. 2** Filler concentration dependent conductivity variation for NCPE films: 15Cu(ClO<sub>4</sub>)<sub>2</sub>·6H<sub>2</sub>O + x Al<sub>2</sub>O<sub>3</sub>. (Inset) Z''-Z' plot for NCPE films: [85PEO + 15Cu(ClO<sub>4</sub>)<sub>2</sub>·6H<sub>2</sub>O] + 2Al<sub>2</sub>O<sub>3</sub> and [85PEO + 15Cu(ClO<sub>4</sub>)<sub>2</sub>·6H<sub>2</sub>O] + 5Al<sub>2</sub>O<sub>3</sub>

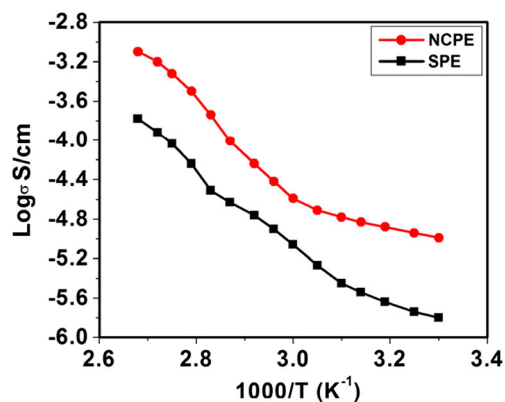


**Fig. 3** “Log σ-1/T” plots for NCPE OCC film: [85PEO: 15Cu(ClO<sub>4</sub>)<sub>2</sub>·6H<sub>2</sub>O] + 2Al<sub>2</sub>O<sub>3</sub> and SPE host film: [85PEO: 15Cu(ClO<sub>4</sub>)<sub>2</sub>·6H<sub>2</sub>O]

Bruker, Germany, CuKα radiation: λ = 1.54 Å), FTIR (IR Affinity-1, Shimadzu Japan), SEM (JSM-IT 300, TouchScope™ scanning electron microscope), DSC (STAR<sup>c</sup>, SW 13.00, METTLER) and TGA (STAR<sup>c</sup> SYSTEM TGA1 SF/1100, METTLER) techniques. Also, from DSC thermal responses, degree of crystallinity (X<sub>c</sub>) has been evaluated with the help of the following equation [25, 26]:

$$X_c = \frac{\Delta H_m}{\Delta H_m^0} \times 100\% \quad (2)$$

where ΔH<sub>m</sub> is the heat enthalpy of pure PEO and salt complexed PEO obtained from the area of respective endothermic peaks, ΔH<sub>m</sub><sup>0</sup> (~213.7 Jg<sup>-1</sup>) is the theoretical value of heat enthalpy for pure PEO with 100% crystalline phase.

## Results and discussion

### Ion transport property characterization

#### Ionic conductivity studies on SPE/NCPE films

Figure 1 shows, the salt concentration (x) dependent conductivity (σ) variation at room temperature (27 °C) on SPE films: [(1-x) PEO: (x) Cu(ClO<sub>4</sub>)<sub>2</sub>·6H<sub>2</sub>O]. It can be clearly noted that the conductivity increased abruptly on initial addition of salt by x = 2 wt% then remained almost unaltered afterward up to x = 25 wt% salt, except for a moderate size conductivity maxima at x = 15 wt% salt. Films beyond 25 wt% appeared mechanically unstable. SPE film: [85PEO: 15Cu(ClO<sub>4</sub>)<sub>2</sub>·6H<sub>2</sub>O], exhibiting relatively higher room temperature conductivity (σ<sub>rt</sub> ~ 1.59 × 10<sup>-6</sup> S/cm) has been chosen as SPE OCC film. Σ<sub>rt</sub> enhancement of approximately three orders of magnitude was obtained in SPE OCC film from that of pure PEO (σ<sub>rt</sub> ~ 3.2 × 10<sup>-9</sup> S/cm). The reason for σ<sub>rt</sub>-increase, as usual, can be attributed to increase in degree of amorphous phase in the

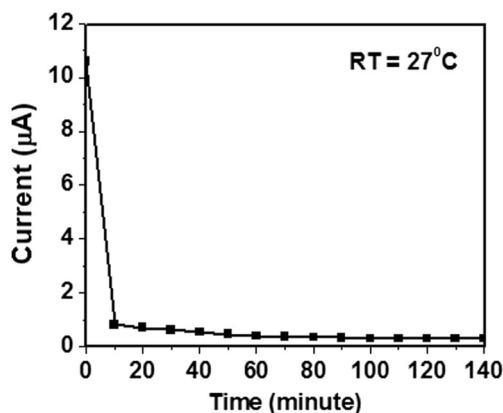
**Table 1** Value of  $\sigma_{rt}$ ,  $t_{ion}$ ,  $t_+$ ,  $E_a$  for NCPE OCC/SPE host films along with  $\sigma_{rt}$  of pure PEO

Film sample (hot-press cast)	$\sigma_{rt}$ (S/cm)	$t_{ion}$	$t_+$	$E_a$ (eV)
Pure PEO	$3.2 \times 10^{-9}$	–	–	–
SPE OCC: [85PEO: 15Cu(ClO <sub>4</sub> ) <sub>2</sub> ·6H <sub>2</sub> O]	$1.59 \times 10^{-6}$	0.98	0.22	0.29
NCPE OCC: [85PEO: 15Cu(ClO <sub>4</sub> ) <sub>2</sub> ·6H <sub>2</sub> O] + 2Al <sub>2</sub> O <sub>3</sub>	$1.76 \times 10^{-5}$	0.99	0.26	0.20

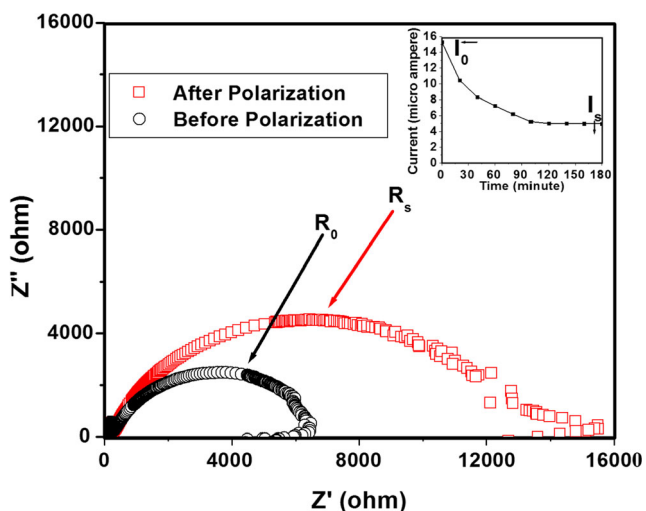
polymeric host due to complexation/dissolution of salt in PEO. The inset in the figure shows the  $Z''$ - $Z'$  plot for SPE OCC films: [85PEO: 15Cu(ClO<sub>4</sub>)<sub>2</sub>·6H<sub>2</sub>O].

Figure 2 shows “log  $\sigma$ - $x$ ” plot for different NCPE films: [85PEO: 15Cu(ClO<sub>4</sub>)<sub>2</sub>·6H<sub>2</sub>O] +  $x$  Al<sub>2</sub>O<sub>3</sub> at room temperature (27 °C). One can clearly notice the appearance of two  $\sigma$ -maxima at  $x=2$  and 5 wt% in “log  $\sigma$ - $x$ ” plot, marked by arrow. However, since the conductivity value of NCPE film for  $x=2$  wt% was relatively higher, this NCPE film: [85PEO + 15Cu(ClO<sub>4</sub>)<sub>2</sub>·6H<sub>2</sub>O] + 2 Al<sub>2</sub>O<sub>3</sub>, with room temperature conductivity ( $\sigma$ )~ $1.76 \times 10^{-5}$  S/cm, has been referred to as NCPE OCC film. Conductivity measurement of the film

sample placed between SS-electrodes was done by A. C. Impedance Spectroscopy (IS) technique using impedance analyzer LCR meter (HIOKI IM – 3533, Japan) in the frequency range: 1 mHz–200 KHz. The inset in the figure shows the  $Z''$ - $Z'$  plots for these two NCPE films: [85PEO: 15Cu(ClO<sub>4</sub>)<sub>2</sub>·6H<sub>2</sub>O] + 2 Al<sub>2</sub>O<sub>3</sub> and [85PEO: 15Cu(ClO<sub>4</sub>)<sub>2</sub>·6H<sub>2</sub>O] + 5 Al<sub>2</sub>O<sub>3</sub>. The existence of two  $\sigma$ -peaks has often been observed in the majority of CPE/NCPE films reported in the past and has been explained on the basis of two percolation model, suggested by Laxmi and Chandra [27]. It has been proposed that two kinds of transport mechanism are operative in these systems. Accordingly, the first  $\sigma$ -maxima is possibly due to the dissociation of ion aggregates and/or undissociated salt which resulted into the generation of free ion



**Fig. 4** “Current-Time” TIC plot for NCPE OCC membrane: [85PEO: 15Cu(ClO<sub>4</sub>)<sub>2</sub>·6H<sub>2</sub>O] + 2 Al<sub>2</sub>O<sub>3</sub>



**Fig. 5**  $Z''$ - $Z'$  complex impedance and “Current-Time” [Inset] plots for NCPE OCC film: [85PEO: 15Cu(ClO<sub>4</sub>)<sub>2</sub>·6H<sub>2</sub>O] + 2 Al<sub>2</sub>O<sub>3</sub>

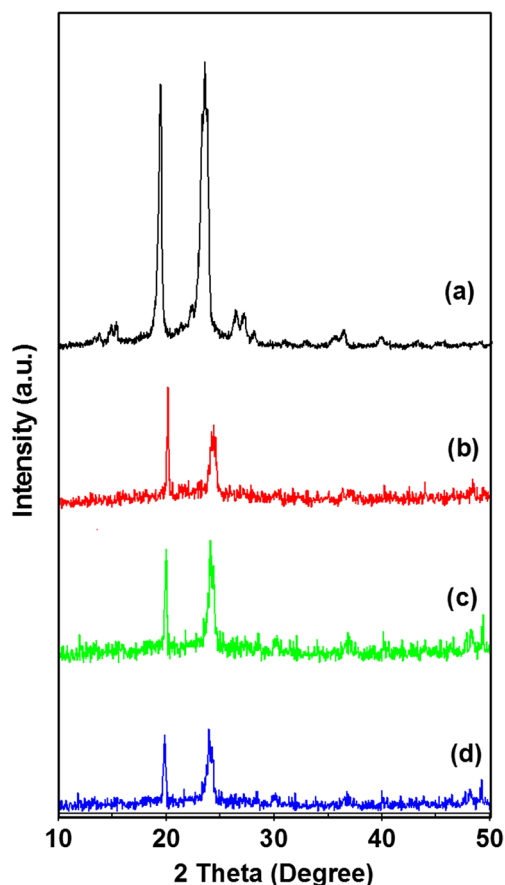


**Fig. 6** XRD pattern for: **a** pure PEO, **b** salt Cu(ClO<sub>4</sub>)<sub>2</sub>·6H<sub>2</sub>O, **c** SPE host film: [85PEO: 15Cu(ClO<sub>4</sub>)<sub>2</sub>·6H<sub>2</sub>O], and **d** NCPE OCC film: [85PEO: 15Cu(ClO<sub>4</sub>)<sub>2</sub>·6H<sub>2</sub>O] + 2 Al<sub>2</sub>O<sub>3</sub>

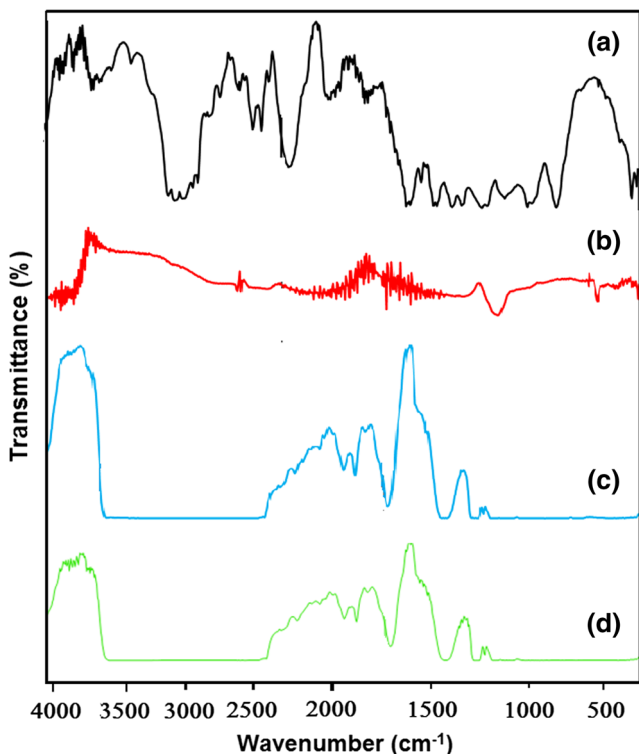


**Fig. 7** FTIR pattern for: **a** pure PEO, **b** salt  $\text{Cu}(\text{ClO}_4)_2 \cdot 6\text{H}_2\text{O}$ , **(c)** SPE host film:  $[\text{85PEO} : 15\text{Cu}(\text{ClO}_4)_2 \cdot 6\text{H}_2\text{O}]$ , and **d** NCPE OCC film:  $[\text{85PEO} : 15\text{Cu}(\text{ClO}_4)_2 \cdot 6\text{H}_2\text{O}] + 2 \text{Al}_2\text{O}_3$

carriers as a consequence of addition of nano-sized  $\text{Al}_2\text{O}_3$  particles. The second  $\sigma$ -maxima as well as the conductivity variation around this ratio is related to the well-known 2-phase composite effect and can be explained on the basis of space-charge and/or percolation model [15, 21].

Table 1 lists  $\sigma_{\text{IT}}$ -value of NCPE OCC film along with that of SPE-host, pure PEO, and the values of  $E_a$ ,  $t_{\text{ion}}$ ,  $t_+$  discussed below. It can be clearly noticed that  $\sigma$ -increase of nearly an order of magnitude was obtained in NCPE OCC film simply after dispersing fractional amount of  $\text{Al}_2\text{O}_3$  nanoparticles into SPE host. Comparing this value with that of pure PEO

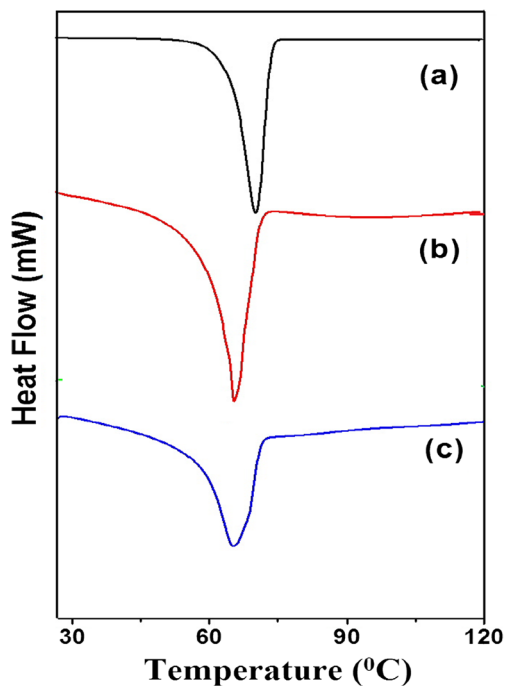


**Fig. 9** DSC pattern for: **a** pure PEO, **b** SPE host film:  $[\text{85PEO} : 15\text{Cu}(\text{ClO}_4)_2 \cdot 6\text{H}_2\text{O}]$ , and **c** NCPE OCC film:  $[\text{85PEO} : 15 \text{Cu}(\text{ClO}_4)_2 \cdot 6\text{H}_2\text{O}] + 2 \text{Al}_2\text{O}_3$

( $\sigma_{\text{IT}} \sim 3.20 \times 10^{-9} \text{ S/cm}$ ), an overall  $\sigma$ -enhancement of nearly four orders of magnitude could be achieved.

**Temperature dependent conductivity study**

Figure 3 shows “ $\log \sigma - 1/T$ ” plot for NCPE OCC film:  $[\text{85PEO} + 15\text{Cu}(\text{ClO}_4)_2 \cdot 6\text{H}_2\text{O}] + 2 \text{Al}_2\text{O}_3$  and SPE host film:  $[\text{85PEO} + 15\text{Cu}(\text{ClO}_4)_2 \cdot 6\text{H}_2\text{O}]$  for direct comparison. One can notice, conductivity initially increased linearly with temperature followed by a slight upward change in the slope around  $\sim 65\text{--}70 \text{ }^\circ\text{C}$ . This temperature region belongs to characteristic semi-crystalline to complete amorphous phase transition of pure PEO which usually occurs at the melting

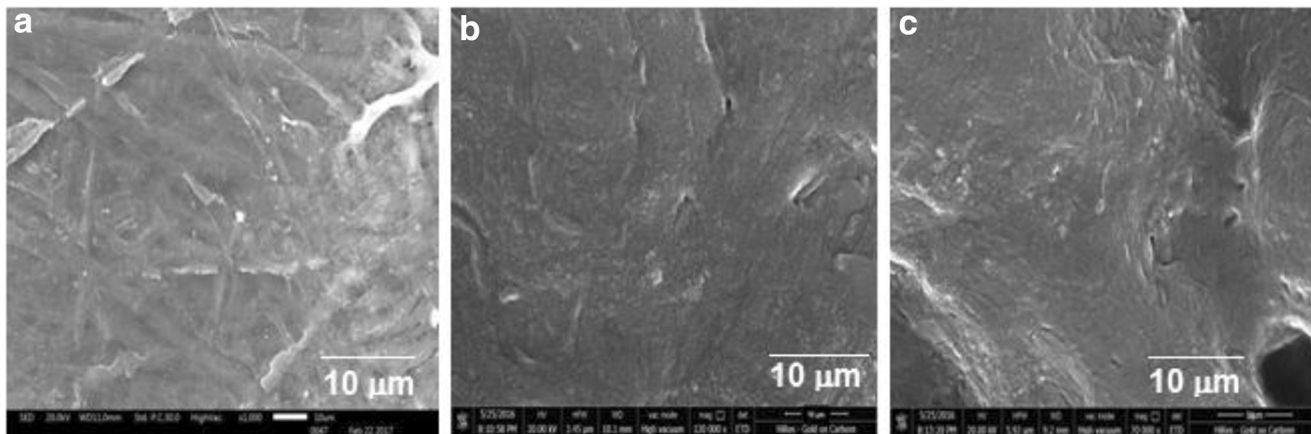


**Fig. 8** SEM images for: **a** pure PEO, **b** SPE host film:  $[\text{85PEO} : 15\text{Cu}(\text{ClO}_4)_2 \cdot 6\text{H}_2\text{O}]$ , and **c** NCPE OCC film:  $[\text{85PEO} : 15\text{Cu}(\text{ClO}_4)_2 \cdot 6\text{H}_2\text{O}] + 2 \text{Al}_2\text{O}_3$

**Table 2** Values of  $T_m$ ,  $\Delta H_m$ , and  $X_c$  for pure PEO, SPE host film: [85PEO: 15Cu(ClO<sub>4</sub>)<sub>2</sub>·6H<sub>2</sub>O] and NCPE OCC film: [85PEO: 15Cu(ClO<sub>4</sub>)<sub>2</sub>·6H<sub>2</sub>O] + 2 Al<sub>2</sub>O<sub>3</sub>

Film sample	$T_m$ (°C)	$\Delta H_m$ (J/g)	$X_c$ (%)
Pure PEO	71.09	175.15	81.90
SPE OCC: [85PEO:15Cu(ClO <sub>4</sub> ) <sub>2</sub> ·6H <sub>2</sub> O]	67.95	96.59	45.20
NCPE OCC: [85PEO: 15Cu(ClO <sub>4</sub> ) <sub>2</sub> ·6H <sub>2</sub> O] + 2Al <sub>2</sub> O <sub>3</sub>	66.95	81.47	38.12

temperature ( $T_m$ ) ~65 °C. “Log  $\sigma$ -1/ $T$ ” plots for both SPE host and NCPE OCC films below this transition region can very well be expressed by Arrhenius straight line equation which is indicative of ion transport via jump/hop mechanism:

$$\text{Log } \sigma = \text{Log } \sigma_0 - \frac{E_a}{kT} \quad (3)$$

where  $\sigma_0$  is the pre-exponential factor,  $k$  is the Boltzmann constant, and  $E_a$  is the activation energy in eV.  $E_a$  value, listed in Table 1 has been computed by linear least square fitting of straight line portion of “Log  $\sigma$ -1/ $T$ ” plot below 60 °C and found ~0.20 eV (NCPE OCC film), ~0.29 eV (SPE host).

### Ionic/cationic transference number studies

Figure 4 shows a typical TIC plot for NCPE OCC film. The total current approached close to zero in about 3 h indicating that the mobile ions in the cell SS //NCPE OCC// SS, subjected to an external dc potential, have been completely polarized at the respective electrode/electrolyte interfaces. TIC plot (not shown here) for SPE host film looked almost alike and  $t_{\text{ion}} \sim 0.98$ .  $t_{\text{ion}}$  value obtained for both the films is very close to unity, hence, indicative of the conductivity which is predominantly ionic. However, in polymer electrolytes, both cations and anions move, and the cationic transport number is a key parameter as regards to the performance of the electrolyte in a battery is concerned. In order to evaluate Cu<sup>2+</sup> – ion transport in the present NCPE system, it was evaluated separately using a combined ac/dc technique and with the help of Eq. (1), as mentioned in section 2. NCPE OCC film, placed between two Cu-metal electrodes, was subjected to an external fixed dc potential ( $\Delta V$ ) = 1 V. The values of  $I_0/I_s$  and  $R_0/R_s$  have been obtained from “Current-Time” and  $Z'$ - $Z''$  complex impedance plots shown in Fig. 5 and its inset, respectively. For SPE OCC film, similar plots (not shown here).  $t_+$  was found to be ~0.26 (NCPE OCC film), ~0.22 (SPE host film) (as listed in Table 1). This clearly indicated that as a consequence of dispersal of Al<sub>2</sub>O<sub>3</sub> passive filler material particles into SPE host,  $t_+$  has been increased quite significantly.

### Materials property characterization

#### XRD and FTIR studies

Figure 6 shows XRD patterns for pure PEO, salt Cu(ClO<sub>4</sub>)<sub>2</sub>·6H<sub>2</sub>O, SPE host film: [85PEO: 15Cu

(ClO<sub>4</sub>)<sub>2</sub>·6H<sub>2</sub>O], and NCPE OCC film: [85PEO: 15Cu(ClO<sub>4</sub>)<sub>2</sub>·6H<sub>2</sub>O] + 2 Al<sub>2</sub>O<sub>3</sub>. Comparison of these patterns clearly confirmed the complexation of salt in the polymeric host, as many of the peaks related to the salt appeared along with PEO peaks, although slightly displaced with decreased intensity. The positions of two main peaks of PEO at  $2\theta \sim 19.3^\circ$  and  $23.3^\circ$  (pattern “a”) remained almost intact even after complexation of salt in PEO in SPE and dispersal of Al<sub>2</sub>O<sub>3</sub> (in NCPE). However, the intensity of PEO main peaks has been suppressed substantially after complexation of salt in PEO (pattern “c”) and/or dispersal of IInd-phase nano-filler particles in SPE host (pattern “d”). Such suppression in peak intensity is usually indicative of decrease in degree of crystallinity and/or increase in degree of amorphosity in polymeric host [20, 25]. This, in turn, supports  $\sigma_{\text{IT}}$ -increase in dry polymer electrolyte systems.

Complexation of salt in PEO has been re-confirmed by FTIR studies. Figure 7 shows FTIR spectra for pure PEO, salt, SPE host film, and NCPE OCC films. The vibrational bands (pattern “a”) at ~2238, ~2163, and ~1963 cm<sup>-1</sup> are characteristic of pure PEO; peaks at ~525–530 and ~1200 cm<sup>-1</sup> are related to C-O-C bending and stretching mode, respectively; bands at ~750–950, ~1820, ~2900–3000, ~1475, ~845 correspond to symmetric/asymmetric stretching/vibration of CH<sub>2</sub> group, CH<sub>2</sub> bending, CH<sub>2</sub> rocking, etc. Significant changes in the spectral response could be noticed after complexation of salt in SPE host (pattern “c”) and/or dispersal of IInd-phase nano-filler particle in SPE host (pattern “d”), which once again confirmed the complexation of salt in PEO.

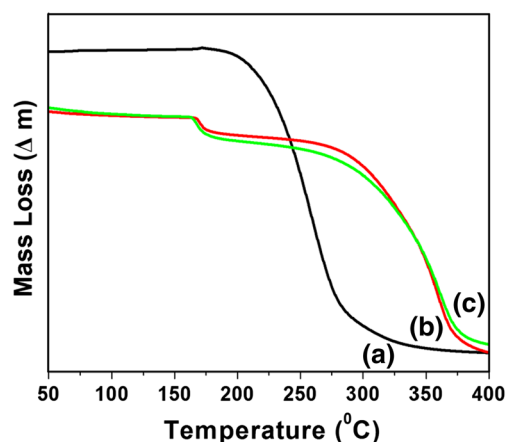


**Fig. 10** TGA for: **a** pure PEO, **b** SPE host film: [85PEO: 15Cu(ClO<sub>4</sub>)<sub>2</sub>·6H<sub>2</sub>O], and **c** NCPE OCC film: [85PEO: 15Cu(ClO<sub>4</sub>)<sub>2</sub>·6H<sub>2</sub>O] + 2 Al<sub>2</sub>O<sub>3</sub>

**Table 3** The values of decomposition temperature and weight loss (%) for pure PEO, SPE host film: [85PEO: 15Cu(ClO<sub>4</sub>)<sub>2</sub>·6H<sub>2</sub>O] and NCPE OCC film: [85PEO: 15Cu(ClO<sub>4</sub>)<sub>2</sub>·6H<sub>2</sub>O] + 2 Al<sub>2</sub>O<sub>3</sub>

Film sample	Decomposition temperature (°C)		Mass loss (Δ m)
	Onset	Endset	
Pure PEO	226.56	282.47	85.33
SPE OCC: [85PEO:15Cu(ClO <sub>4</sub> ) <sub>2</sub> ·6H <sub>2</sub> O]	326.23	371.24	79.54
NCPE OCC: [85PEO: 15Cu(ClO <sub>4</sub> ) <sub>2</sub> ·6H <sub>2</sub> O] + 2Al <sub>2</sub> O <sub>3</sub>	325.58	373.99	72.79

## SEM study

Figure 8 shows SEM surface images for pure PEO, SPE host film: [85PEO: 15Cu(ClO<sub>4</sub>)<sub>2</sub>·6H<sub>2</sub>O] and NCPE OCC film: [85PEO: 15Cu(ClO<sub>4</sub>)<sub>2</sub>·6H<sub>2</sub>O] + 2 Al<sub>2</sub>O<sub>3</sub>. The surface morphology for all the films appeared quite smooth with uniform distribution of salt in PEO and/or filler particles in SPE film. There are a few wrinkles present which are probably due to stress field developed during hot-pressing and/or drying of the film.

## DSC and TGA study

Figure 9 shows DSC thermo-grams for pure PEO, SPE host film: [85PEO: 15Cu(ClO<sub>4</sub>)<sub>2</sub>·6H<sub>2</sub>O] and NCPE OCC film: [85PEO: 15Cu(ClO<sub>4</sub>)<sub>2</sub>·6H<sub>2</sub>O] + 2 Al<sub>2</sub>O<sub>3</sub>. The sharp endothermic peak (curve “a”) at ~71.09 °C belongs to characteristic semi-crystalline to complete amorphous phase transition temperature ( $T_m$ ) of pure PEO. As a consequence of complexation of salt in PEO and/or dispersal of nanoparticles of active filler in SPE host, the peak position sifted slightly toward lower temperature region ~67.95 °C (curve “b”), ~66.95 °C (curve “c”), respectively. Also, the area of endothermic peak decreased significantly. These changes are also often considered as confirmation of complexation of salt in PEO and/or dispersal of filler material in SPE host. The reduction in peak area relates to decrease in degree of crystallinity in PEO. The relative percentage of crystallinity ( $X_c$ ) in PEO as well as in SPE host and NCPE OCC films has been evaluated with the help of Eq. (2), mentioned in section 2 and listed in Table 2 along with  $T_m$  and  $\Delta H_m$  values. As a consequence of complexation of salt in pure PEO and/or dispersal of filler material in SPE host, it can be clearly noticed that degree of crystallinity/degree of amorphosity in PEO has substantial decreased/increased which also support our XRD results, discussed in subsection 3.2.1.

Figure 10 shows TGA curves for pure PEO, SPE host film: [85PEO: 15Cu(ClO<sub>4</sub>)<sub>2</sub>·6H<sub>2</sub>O] and NCPE OCC film: [85PEO: 15Cu(ClO<sub>4</sub>)<sub>2</sub>·6H<sub>2</sub>O] + 2 Al<sub>2</sub>O<sub>3</sub>. Table 3 lists the values of decomposition temperature and mass loss (Δ m) obtained from TGA study. On comparing, one can clearly note that after complexation of salt and/or dispersal of filler particles, the thermal stability of polymer improved significantly with substantial decrease in mass loss (Δ m).

## Conclusion

The motivation of this work is preparing lithium-free chemical-based solid state battery due to safety issues caused by lithium chemical, a new non-lithium chemical-based Cu<sup>2+</sup>-conducting nano-composite polymer electrolyte (NCPE): [85PEO: 15Cu(ClO<sub>4</sub>)<sub>2</sub>·6H<sub>2</sub>O] + 2 Al<sub>2</sub>O<sub>3</sub> has been investigated. NCPE film has been prepared by hot-press cast technique using SPE composition: [85PEO: 15Cu(ClO<sub>4</sub>)<sub>2</sub>·6H<sub>2</sub>O] as Ist-phase host and nanoparticles of active filler material Al<sub>2</sub>O<sub>3</sub> as IInd-phase dispersoid. SPE used here as Ist-phase host exhibited  $\sigma_{rt}$ -enhancement of nearly three orders of magnitude from that of pure PEO. Dispersal of IInd-phase into Ist-phase increased  $\sigma_{rt}$  further by approximately an order of magnitude. An overall increase of ~4 orders of magnitude in  $\sigma_{rt}$  could be achieved in NCPE film. Ionic transference ( $t_{ion}$ ) studies indicated that both SPE host/NCPE film materials predominantly ionic with cation transference number ( $t_+$ ) ~0.26 which has increased significantly after dispersal of filler material particles in SPE host. Complexation of salt in PEO and/or dispersal of IInd-phase into Ist-phase has been confirmed by XRD, FTIR, SEM, DSC, and TGA studies. The battery performed satisfactorily during low current drain.

## References

- Fenton DE, Parker JM, Wriugh PV (1973) Complexes of alkali metal ions with poly(ethylene oxide). *Polymer* 14(11):589. [https://doi.org/10.1016/0032-3861\(73\)90146-8](https://doi.org/10.1016/0032-3861(73)90146-8)
- Armand MP, Chabagno JM, Diadat M (1979) Fast ion transport in solids. In: Vashistha P, Mundy JM, ShenY GK (Eds), North Holland, p 131
- Armand MB (1986) Polymer electrolytes. *Annu Rev Mater Sci* 16(1):245–261. <https://doi.org/10.1146/annurev.ms.16.080186.001333>
- Ratner MA, Shriver DF (1988) Ion transport in solvent-free polymers. *Chem Rev* 88(1):109–124. <https://doi.org/10.1021/cr00083a006>
- Mac Callum JR, Vincent CA (eds) (1987 & 1989) *Polymer electrolyte reviews*, 1, 2. Elsevier Applied Science Publisher, London
- Murata K (1995) An overview of the research and development of solid polymer electrolyte batteries. *Electrochim Acta* 40(13-14): 2177–2184. [https://doi.org/10.1016/0013-4686\(95\)00160-G](https://doi.org/10.1016/0013-4686(95)00160-G)
- Bruce PG (ed) (1995) *Solid state chemistry*. Cambridge University Press, Cambridge

8. Gray FM, Connor JA (eds) (1997) Polymer electrolytes (RSC materials monographs). Royal Society of Chemistry, Cambridge
9. Capuano F, Croce F, Scrosati B (1991) Composite polymer electrolytes. *J Electrochem Soc* 138(7):1918. <https://doi.org/10.1149/1.2085900>
10. Croce F, Appetecchi GB, Persi L, Scrosati B (1998) Nanocomposite polymer electrolytes for lithium batteries. *Nature* 394(6692):456–458. <https://doi.org/10.1038/28818>
11. Appetecchi GB, Croce F, Persi L, Ronci F, Scrosati B (2000) Transport and interfacial properties of composite polymer electrolytes. *Electrochem Acta* 45(8-9):1481–1490. [https://doi.org/10.1016/S0013-4686\(99\)00363-1](https://doi.org/10.1016/S0013-4686(99)00363-1)
12. Appetecchi GB, Hassoun J, Scrosati B, Croce F, Cassel F, Salomon M (2003) Hot-pressed, solvent-free, nanocomposite, PEO-based electrolyte membranes. *J Power Sources* 124(1):246–253. [https://doi.org/10.1016/S0378-7753\(03\)00611-6](https://doi.org/10.1016/S0378-7753(03)00611-6)
13. Agrawal RC, Chandra A (2007) *J. Physics D. Appl Phys* 40:7024
14. Pandey GP, Hashmi SA, Agrawal RC (2008) Hot-press synthesized polyethylene oxide based proton conducting nanocomposite polymer electrolyte dispersed with SiO<sub>2</sub> nanoparticles. *Solid State Ionics* 179(15-16):543–549. <https://doi.org/10.1016/j.ssi.2008.04.006>
15. Agrawal RC, Bhatt A, Mahipal YK (2008) Investigations on ion transport properties of and battery discharge characteristic studies on hot-pressed Ag<sup>+</sup>-ion-conducting nano-composite polymer electrolytes: (1-x) [90PEO : 10AgNO<sub>3</sub>] : xSiO<sub>2</sub>. *New J Phys* 10(4):043023. <https://doi.org/10.1088/1367-2630/10/4/043023>
16. Agrawal RC, Pandey GP (2008) *J Phys D Appl Phys* 41:055409
17. Chandra A, Agrawal RC, Mahipal YK (2009) Ion transport property studies on PEO–PVP blended solid polymer electrolyte membranes. *J Phys D Appl Phys* 42(13):135107. <https://doi.org/10.1088/0022-3727/42/13/135107>
18. Pandey GP, Agrawal RC, Hashmi SA (2010) *J Phys D Appl Phys* 43:25550
19. Agrawal RC, Mahipal YK, Ashrafi R (2011) Materials and ion transport property studies on hot-press casted solid polymer electrolyte membranes: [(1-x) PEO: x KIO<sub>3</sub>]. *Solid State Ionics* 192(1):6–8. <https://doi.org/10.1016/j.ssi.2010.05.048>
20. Agrawal RC, Pandey GP (2008) *J. Phys. D: Appl Phys* 41:223001 (Topical Review)
21. Agrawal RC, Gupta RK (1999) Superionic solids: composite electrolyte phase—an overview. *J Mater Sci* 34(6):1131–1162. <https://doi.org/10.1023/A:1004598902146>
22. Chandra S, Tolpadi SK, Hashmi SA (1988) *Solid State Ionics* 28–30:615
23. Watanabe M, Sanui K, Ogata N, Kobayashi T, Ontaki Z (1985) Ionic conductivity and mobility in network polymers from poly(propylene oxide) containing lithium perchlorate. *J Appl Phys* 57(1):123–128. <https://doi.org/10.1063/1.335386>
24. Evans J, Vincent CA, Bruce PG (1987) Electrochemical measurement of transference numbers in polymer electrolytes. *Polymer* 28(13):2324–2328. [https://doi.org/10.1016/0032-3861\(87\)90394-6](https://doi.org/10.1016/0032-3861(87)90394-6)
25. Shin JH, Henderson WA, Passerini S (2003) Ionic liquids to the rescue? Overcoming the ionic conductivity limitations of polymer electrolytes. *Electrochem Commun* 5(12):1016–1020. <https://doi.org/10.1016/j.elecom.2003.09.017>
26. Ibrahim S, Johan MR (2012) *Int. J. Electrochem.Sci* 7:–2596
27. Laxmi N, Chandra S (2001) *Phys. Stat. Solid (a)* 186:–395
28. Quartarone E, Murtarelli P (2011) *Chem Soc Rev* 40:2025
29. Agrawal RC (2013) Technical proc. NSTI nano technology conf. & expo. *Nanotech* 2:–650
30. Karan S, Sahu TB, Sahu M, Agrawal RC (2015) *Materials Today Proceeding* 3:109
31. Agrawal RC, Sahu DK, Mahipal YK, Ashrafi R (2013) *Matl. Chem Phys* 139:410
32. Agrawal RC, Sahu DK, Mahipal YK, Ashrafi R (2012) *Ind. J. Pure and App. Physics*
33. Karan S, Sahu TB, Sahu M, Mahipal YK, Agrawal RC (2017) *Ionics* (2017) 23:–2721
34. Dissanayake MAKL, Jayathilaka PARD, Bokalawela RSP (2005) Ionic conductivity of PEO<sub>9</sub>: Cu(CF<sub>3</sub>SO<sub>3</sub>)<sub>2</sub>: Al<sub>2</sub>O<sub>3</sub> nanocomposite solid polymer electrolyte. *Electrochim Acta* 50(28):5602–5605. <https://doi.org/10.1016/j.electacta.2005.03.038>
35. Dissanayake MAKL (1989) Solid state cells with mixed polycrystalline CuCl–CuCNS electrolyte and Mg/Cu electrodes. *Solid State Ionics* 34(4):257–259. [https://doi.org/10.1016/0167-2738\(89\)90452-9](https://doi.org/10.1016/0167-2738(89)90452-9)
36. Magistris A, Chiodelli G, Sing K, Ferloni P (1990) Electrical and thermal properties of PEO Cu(ClO<sub>4</sub>)<sub>2</sub> polymer electrolytes. *Solid State Ionics* 38(3-4):235–240. [https://doi.org/10.1016/0167-2738\(90\)90427-S](https://doi.org/10.1016/0167-2738(90)90427-S)
37. Sahu TB, Sahu M, Karan S, Mahipal YK, Sahu DK, Agrawal RC (2017) Synthesis and characterization of ion transport behavior in Cu<sup>2+</sup>-conducting nano composite polymer electrolyte membranes. *J Phys D Appl Phys* 50(27):275501. <https://doi.org/10.1088/1361-6463/aa7527>